IDEAL MHD STABILITY PROPERTIES OF PRESSURE-DRIVEN

MODES IN LOW SHEAR TOKAMAKS

J. Manickam and N. Pomphrey

Princeton Plasma Physics Laboratory

Princeton, New Jersey 08544

and

A.M.M. Todd

Grumman Corporation

Plainsboro, New Jersey 08536

Abstract

The role of shear in determining the ideal MHD stability properties of

tokamaks is discussed. In particular, we assess the effects of low shear

within the plasma upon pressure-driven modes. The standard ballooning theory

is shown to break down, as the shear is reduced and the growth rate is shown

to be an oscillatory function of n, the toroidal mode number, treated as a

continuous parameter. The oscillations are shown to depend on both the

pressure and safety-factor profiles. When the shear is sufficiently weak, the

oscillations can result in bands of unstable n values which are present even

when the standard ballooning theory predicts complete stability. These

instabilities are named "infernal modes." The occurrence of these

instabilities at integer n is shown to be a sensitive function of q-axis,

raising the possibility of a sharp onset as plasma parameters evolve.

MASTER

Introduction

The importance of shear in determining the ideal MHD stability properties of tokamaks is well recognized. The general understanding of its role was largely based on simple cylindrical models, e.g., the review articles of Wesson [1] and Friedberg [2]. More recently is has become clear that careful numerical treatment is essential to define its effects on the stability of ideal MHD modes [3-8]. This understanding has been used to propose paths to second regions of stability [9-10]. However, there remain areas of imperfect understanding, one of which we intend to explore in this report. In particular, we assess the role of low shear on the stability of pressure-driven modes. The shear generally refers to a gradient in the safety-factor profile. In some situations it is represented by the ratio of q-edge to q-axis, it may also be defined as ψ dq/dψ ($\equiv\psi$q'), which will be referred to here as the global shear. Another form that plays an important role in high-n ballooning modes is the local shear, a quantity which measures the skewness of the magnetic field lines on nearby surfaces, and which has been identified as playing a critical role in determining stability to ballooning modes [7].

In this report we shall be largely concerned with the global shear and its effect on internal pressure-driven instabilities. These modes have been analyzed extensively using analytical and numerical methods. In general, when the toroidal mode number, n, is large, the ballooning theory [11-13] is applicable. In this approach it is observed that ballooning modes may be constructed from the overlap of many localized Fourier modes peaking on their own rational surfaces. In the high-n limit this also implies a radial localization of the mode, which permits the reduction of the equations to an ordinary differential equation valid on each flux surface. Thus each flux surface can be independently tested for stability to high-n ballooning

modes. In contrast, when n is small (~1), the numerical approach of solving the full two-dimensional ideal MHD equations [14-15] is required. This latter approach can, in principle, be extended to high-n. However, in practice, mode resolution and hence computer memory requirements restrict the analysis to n $\leq$ 10. The ballooning theory has been modified to include finite-n corrections, and has been shown to agree with the detailed MHD approach down to n ~ 5 [16-18]. Ballooning theory predicts that the largest n modes are the most unstable, and that as n is decreased the growth rate decreases monotonically. In certain circumstances this picture is modified to include an oscillatory dependence of growth rate on mode number. This was shown explicitly in Ref. 16 where n was treated as a continuous variable. The oscillatory behavior has been independently described by Hastie and Taylor [19] who attribute the oscillations to a breakdown of the standard ballooning theory when the global shear becomes weak. They also propose a new theory which would supercede the standard ballooning theory in these conditions. They postulate regions of validity of their theory and show that in the high-n limit the standard ballooning theory is recovered. This article addresses itself to the same problem. In particular, we verify the Hastie-Taylor theory when the shear is weak, and we shall also show that if the shear is further reduced, that even this theory breaks down; instabilities are observed, which can be present even when the standard ballooning theory predicts complete stability. We name these instabilities "infernal modes." We shall discuss them and analyze the role of both p' ($\equiv$ dp/dψ) and q' in driving the instability.

Weak shear near the axis is often accompanied by strong shear near the plasma edge which has a strong stabilizing influence on the external kink mode. In this situation the threshold for instability can be at very large

values of β, ($\equiv 2 <p>/<B^2>$) and the instability can take the form of an internal mode, where the boundary conditions play a minor role in determining stability. In particular, when q' is small and p' is large near the axis, the resulting instability may be dominated by a low-m (~1) Fourier component, even when there is no q = 1 surface inside the plasma. This is significant, in that it represents a fairly typical operating scenario for tokamaks suggesting that these instabilities may play an important role in present high-β tokamaks.

In the following sections we shall describe the equilibrium models and numerical methods used in this study. We then present our results, highlighting several of the issues raised here. Finally, we present our observations and conclusions.

Equilibrium Model and Numerical Methods

This study focuses on the role of the shear on stability to pressure-driven modes. Since these are essentially profile-related effects, we choose a simple geometry for the plasma, and consider a circular cross-sectional tokamak with an aspect ratio, R/a = 4. The q-profile is specified to have the functional form

$$q = q_0 + q_1 \, \psi^{\alpha}q \quad ,$$

so that q_0 determines q-axis, and q-edge = $q_0 + q_1$. We have chosen $q_0 = 1.05$, and $q_1 = 2.05$ for the majority of cases studied here - the exceptions will be noted. The flux label, ψ, is normalized to have a value of zero at the magnetic axis and unity at the plasma edge, α_q is used to vary the shear. When α_q is greater than unity, which is the case for this study, the shear has

its minimum near the axis. If q-axis and q-edge are held fixed, as α_q is increased the effect is to weaken simultaneously the shear near the axis and increase the shear near the edge. Figure 1 shows the q-profile for several values of α_q. The main body of the results requires a large pressure gradient in regions of low shear, hence we adopt a pressure profile of the form

$$p = p_0 \; (1-\psi^{\alpha_2})^{\alpha_1}$$

with $\alpha_1 = 4$, and $\alpha_2 = 1.5$. The central pressure, p_0, is adjusted to yield the desired value of β. The profile and its derivative are shown in Fig. 2a. We choose β so that, as α_q is varied the resulting equilibria remain unstable to ballooning modes. A convenient choice, for our study, is to set β equal to 1.5%. The equilibrium calculations are made with a flux coordinate solver [20] on a mesh with 50 radial and 100 poloidal intervals. This is then interpolated onto a finer grid with 200 radial and 128 poloidal intervals for the stability analysis which is conducted using the PEST code [14]. This mesh is also used for the standard WKB-ballooning code [16]. In this study we consider toroidal mode numbers up to 12, which requires an ability to resolve poloidal harmonics with a value up to 40. To ensure this resolution, at the higher values of n, we double the number of poloidal mesh points up to 256. An examination of the resulting eigenvectors shows the adequacy of these meshes. Finally, we note that, since we intend to compare eigenvalues of different toroidal modes, we cannot use the scalar version of PEST [21], and must use the proper kinetic energy normalization of the complete representation [14].

Our procedure is to generate several equilibria for different values of α_q keeping β equal to 1.5%, and then analyze them for stability to ballooning

modes. A conducting shell is placed at the plasma edge and the radial perturbation is required to vanish there. We utilize the WKB code to determine the stability properties according to the standard ballooning theory, including predictions of the critical-n for instability using the quantization condition where applicable. We then analyze the same equilibria using the PEST code, treating the toroidal mode number, n, as a continuous real variable, rather than an integer. This is justified by the fact that n appears as a fixed expansion parameter in the ballooning theory. Further, it generally appears in stability analysis as a product of n with q, and we can interpret noninteger n for a certain value of q, as an integer n for a slightly modified q-profile. We plot the growth rate as a function of n and compare the results with the predictions of the different ballooning theories.

Results

The PEST code, being an exact code with no approximations or orderings, will be used to represent the true situation. We will then compare the results of the ballooning mode analysis with the PEST results. We commence with a case which conforms to standard ballooning theory. For this we choose α_q equal to 1.5, $\beta \sim 0.8\%$, and the pressure-profile is that of Fig. 2a. Figure 3a shows the results from the PEST-II code [21], where we plot the growth rate as a function of n. (The PEST-II code has been used here as we are only looking for the point of marginal stability; in all subsequent studies we use the PEST-I code [14].) An extrapolation to zero growth rate shows a critical-n of 5.6. The results of a ballooning mode analysis are shown in Fig. 3b, where we plot contours of constant growth rate λ in the $\psi-\theta_k$ plane; θ_k represents the angle between the radial component of the wave-vector, k_q, and the component parallel to the field line, k_α. Details of this

can be found in Ref. 16. In this report we plot $\lambda(\psi, \theta_k)$ rather than $\lambda(q, \theta_k)$ to enhance the visibility of the unstable regions. Using a WKB quantization condition it is then possible to determine the value of the n-crit above which the mode is unstable. In this example the critical-n has the value 5.7, which is in virtual coincidence with the value predicted by the PEST analysis. This confirms the general validity of the codes and procedures used in this study, and reaffirms the possibility of correctly analyzing moderate-n ballooning modes in a standard situation with both the ballooning and PEST codes. We now proceed to the analysis of weak shear equilibria.

The role of the shear is central to these results, hence we fix the pressure profile and adjust p_0 such that β remains approximately constant with a value of 1.5%. We then vary the shear profile parameter α_q over a wide range to modify the shear. The results are shown in a form similar to that of Fig. 3. In each case we show the variation of the growth rate in units of the poloidal Alfven frequency, as obtained from the PEST code, with the toroidal mode number, n. Corresponding to the PEST analysis we also show the ballooning code analysis as contours in the ψ-θ_k plane. It will be noted that some of the contours appear as open lines when a separatrix is present. In this situation the usual method of determining n-crit from the area of the closed contour corresponding to $\lambda = 0$ breaks down, and the n-crit reported must be considered as approximate. The results for α_q equal to 1.1, 1.5, 2, 2.5, 3, 4, and 6 are shown in Figs. 4, 5, 6, 7, 8, 9, and 10, respectively. The PEST results for this sequence of equilibria show a distinct progression from a relatively smooth monotonic dependence of the growth rate on n, to a strongly oscillatory function, which eventually leads to alternating stable and unstable bands in n. We attribute this to the gradual reduction of the shear, q', in the vicinity of the driving force, the pressure gradient. We

note that when α_q is less than 3, that for n larger than 5, there is a monotonic variation of the growth-rate, and for smaller values of n there are oscillations. This result is in agreement with the low-shear theory of Ref. 19; which predicts that when q' is small there exists a critical value of n above which standard ballooning theory would apply, and below this value one would expect oscillations in the growth rate. This general picture is clearly supported here and will be addressed in greater detail below. As α_q increases, the oscillations are extended to larger values of n: the PEST code is limited to n-values of about 10, hence the expected monotonic variation at high-n is not observed in these cases.

The ballooning analysis of these equilibria shows a distinct topological change in the constant λ contours as α_q is increased. We note that the region of instability extends to θ_k equal to π, and a separatrix appears. In Ref. 16 it was argued that the appearance of this separatrix was responsible for the oscillations in the growth rate, which would peak whenever a rational surface coincided with q_x, the surface corresponding to the separatrix. Figure 5 shows that mild oscillations can be present even when there is no separatrix. We believe this is due to the high β value which, for this α_q, is considerably higher than the threshold value for marginal stability. This characteristic appearance of a separatrix is an extremely useful diagnostic for detecting the presence of oscillations. Finally, in relation to this set of figures we comment that when the oscillations are limited in size and range there is some agreement between the n-crit determined by the PEST and WKB-ballooning codes. When α_q is 3 or greater and the oscillations are strong, there is no correlation whatever between the two. In fact, the concept of n-crit is itself questionable.

We have explored the role of the shear in determining the conditions for oscillations. We now analyze the role of the pressure profile. The profile used in the first set of equilibria has its largest gradient at ψ of approximately 0.2, as shown in Fig. 2a. This is also the region where the shear is reduced the most as α_q is changed. We now choose the pressure profile so that it peaks further out, nearer to the plasma edge, by setting α_1 = 2.0 and α_2 = 6.0. This puts the maximum of p' at ψ = 0.9, as shown in Fig. 2b. The q-profile is chosen to be the same as the one analyzed in Fig. 9, with α_q = 4. Figure 11 shows the stability analysis of this equilibrium. Figure 11a shows the PEST results and Fig. 11b the ballooning results. These are to be compared with Fig. 9. The oscillations have disappeared completely and we recover a smooth monotonic dependence of the growth rate on n. This suggests that to get the oscillations it is necessary to have both low shear as well as a large enough p' in the regions of low shear. In fact, based on the results of Figs. 3 and 5, which were for the same q and pressure profile shapes, and differ only in the β (0.8% and 1.5%, respectively), we note that even if q' is moderate, the oscillations can be made to appear if β is increased. However, once instability is reached, it is irrelevant to increase β any further, and the issue of oscillations at higher β is of academic interest. On the other hand, if the oscillations are present close to the threshold of instability, they may have practical consequences. This will become apparent when we study an equilibrium that is stable to infinite-n ballooning modes. We do this by choosing an equilibrium with parameters similar to those of Fig. 10, (i.e., pressure profile of Fig. 2a and α_q = 6), and reducing β until we obtain stability to ballooning modes: this occurs at β = 1%. This equilibrium is then analyzed to obtain the results shown in Fig. 12. Since this is stable to ballooning modes with n = ∞, there is no $\psi-\theta_k$

contour plot. We note the existence of unstable bands at low-n which vanish when n gets sufficiently large. This represents a case where the ballooning mode results would be misleading, as they would infer stability, when in fact there are several low-n internal pressure-driven "ballooning-like" modes. The modes which persist even after the high-n modes are stabilized are termed "infernal-modes."

The results presented here have used a simple parametrization of the q-profile. This form has the disadvantage that the shear throughout the plasma is controlled by a single parameter. Thus, if the shear near the axis is reduced, this increases the shear near the edge. We now introduce a parametrization of q which has the form

$$q = q_0 + q_1 \, \psi^{\alpha_q} \qquad\qquad \text{for } 0 < \psi < \psi_m$$

$$q = q_0 + q_1 \, \psi^{\alpha_q} + q_2 (\psi - \psi_m)^{\alpha_{q2}} \qquad \text{for } \psi_m < \psi < 1 \quad .$$

This form permits us to lower the shear in the region $0 < \psi < \psi_m$, without requiring a large shear outside it, and can more closely represent experimental profiles. In Fig. 13, we show the q, p, and J_ϕ profiles as a function of the distance from the major axis for this profile when q_0, q_1, q_2, α_q, α_{q2}, and ψ_m have the values 1.05, 0.15, q_2, 1.1, 2.8, and 0.3, respectively. Note that the value of q_2 is adjusted so that q-edge = 3.1. The pressure profile parameters are the same as those used earlier, i.e., α_1 = 4 and α_2 = 1.5. With p_0 adjusted to give β = 1.45%, we find the ω^2 dependence shown in Fig. 14a, and the ballooning stability shown in Fig. 14b. As before we note the presence of the separatrix and the sharp resonances in the growth rate for particular values of n. The peaks do not coincide with integer n

and, in fact. only $n = 1$ and $n = 2$ are found to be unstable. At lower β, (0.8%), the ballooning mode is stable; however, the infernal modes are seen to persist, as shown in Fig. 15. To demonstrate the relevance of these infernal modes, we note that when the q is modified slightly, the resonances can destabilize several integer values of n. Figure 16 shows the growth rates for the case of Fig. 15 with the toroidal field scaled so that q-axis changes from 1.05 to 0.96. We note that in this situation several integer n-values are simultaneously destabilized.

The infernal modes add a new wrinkle to the estimation of beta limits. Traditionally, beta limits have been calculated from an analysis of the $n = 1$ external kink and the high-n ballooning instabilities; low- and intermediate-n modes have been largely ignored. This study indicates that such an approach may not be adequate. To illustrate this, we determine the beta limit for a toroidal mode number near the peak of the resonance between $n = 1$ and $n = 2$, i.e., ~1.8, for the sequence of q-profiles studies in Figs. 5-10. This beta limit is compared with that of the high-n ballooning mode in Fig. 17. For a_q > 2, the low-n mode is seen to have a significantly lower threshold. We also note that in this case the toroidal mode numbers with n corresponding to the higher resonances have thresholds which lie between that for $n = 1.8$ and $n = \infty$. The region between the two curves marks the domain of the infernal mode. Finally, Figs. 18 and 19 show plots of the displacement vector field for two typical infernal modes with $n = 3$ and 7. The low-n mode is seen to be broad in its radial extent and may be expected to affect the plasma drastically. The higher-n mode is, however, more localized in its radial extent and the usual understanding of the ballooning mode may apply here.

Discussion

Pressure-driven internal modes in tokamaks have been shown to exhibit a rich complexity if the global shear is weak. Hastie and Taylor have pointed to this in their work and identify two regimes of interest. When n and q' satisfy the relation, $n \gg (\psi q')^{-2} \gg 1$, they predict that the standard ballooning theory is valid. When the shear is reduced so that $(\psi q')^{-2} \gg n \gg 1$, they indicate a need for their new theory. The significant features of their theory are that the growth rate will be an oscillatory function of n with decreasing amplitude, and that when n is large enough to recover the first condition, the results match the standard ballooning theory. The period of the oscillations is predicted to be constant in $n(\Delta n \sim 1/q)$, but the amplitude decreases as $1/n^2$. To determine the region of validity of each of these theories, we plot $(\psi q')^{-2}$ as a function of the radial location in the plasma for different values of α_q in Fig. 20. Since the gradient in the pressure profile peaks at $\psi \sim 0.2$, it is relevant to concentrate on that surface. We note that for $\alpha_q \leq 2$ at $\psi = 0.2$ the value of $(\psi q')^{-2}$ is ~ 1, and we might expect the standard theory to be valid for all $n \gg 1$. This is supported by the results of Figs. 3-6. As α_q is increased from 2 to 3, $(\psi q')^{-2}$ increases sharply from 1.5 to 15. This gives us the conditions to test the Hastie-Taylor theory. In fact, when $\alpha_q = 2.5$ we have observed that when n is greater than 10, the oscillations in $\omega^2(n)$ are damped and a monotonic variation is recovered as predicted. This is partly shown in Fig. 7 which is restricted to $n < 8$, but clearly shows a diminishing amplitude of oscillation. The reduction in the amplitude does not exactly match the predictions of the Hastie-Taylor theory. At small values of n the amplitude decreases slower than $1/n$, and as n is increased it approaches the predicted $1/n^2$. However, for $\alpha_q > 3$, we see no evidence of a reduction in the amplitude

of the oscillation and even the Hastie-Taylor theory breaks down as we enter
the infernal mode regime. It is important to note that it is the value of
$(\psi q')^{-2}$ at the surface of largest p' that matters, not α_q itself. This is
evident from the results of Fig. 11, where p' was chosen to peak at ψ - 0.9, a
surface at which $(\psi q')^{-2} \ll 1$. For this case we note an absence of the
oscillations in $\omega^2(n)$.

In summary, for the model profiles chosen we have shown that when the
shear is moderate so that $(\psi q')^{-2} \leq 1$ at the surface where the pressure has
its maximum gradient, then standard ballooning theory is valid. There is a
monotonic variation of $\omega^2(n)$ and there is also a reasonable correspondence
with the higher order theory which predicts the critical-n. At lower shear
when $1 \leq (\psi q')^{-2} < 10$, the Hastie-Taylor theory is substantially correct.
Oscillations in $\omega^2(n)$ are observed which have a constant period in n.
However, the reduction in the amplitude is slower than predicted except at
larger values of n. When $(\psi q')^{-2} \geq 10$, there is no correspondence with any
existing theory. Oscillations exist in $\omega^2(n)$ but the variation in the
amplitude is completely different, in that there is no evidence of recovering
the standard theory. This may also be noted from the sharp reduction of the
β-limit well below that of the infinite-n theory. In this region we have
infernal modes, which are defined here to be low-n internal pressure-driven
"ballooning" modes which are not described by the standard ballooning
theory. These modes may exist at noninteger n, but are still significant
since they can be induced at integer values of n in a neighboring equilibrium
with a slightly different safety-factor profile. These limited bands of
instability appear to pose a severe problem in determining β-limits. It would
appear necessary to examine several n-values to find the most unstable value
and its corresponding β limit. However, our experience indicates that close

to marginal stability, the most unstable n lies between 1 and 2. Further, we have noted that if the β is high enough to destabilize the high-n ballooning mode, then a separatrix appears in the $\lambda(q,\theta_k)$ contours, and the q_x value corresponding to the location of the separatrix plays an important role in determining the resonances in the $\omega^2(n)$ plot. A practical scheme that would identify the infernal mode β limit, would involve evaluation of $(\psi q')^{-2}$ in the vicinity of the maximum pressure gradient, examination of $\lambda(q,\theta_k)$ contours for an unstable equilibrium to determine q_x, and finally a limited study for n in the range $m/q_x \pm 0.2$, where $m = 1$ or 2. This would identify the most unstable n-value, for which a β-limit may then be determined.

We now comment on the possible relationship with other ideal MHD instabilities. The low-n infernal modes may have a connection with the interchange mode, or the internal kink. The standard Mercier criterion is frequently satisfied here, however its validity when q' vanishes is not obvious. This remains an area open to study. The connection to the internal kink mode is less obvious when we observe that the instability does not seem to require a rational surface in the plasma. Thus when n=1 and even though (nq_{axis}) is greater than unity, we observe an instability with a large m=1 content. However, previous studies [8,22] have shown a connection between the internal kink mode and a low-n (= 1) ballooning-like mode. Hence this avenue remains open for exploration. Finally, we speculate on the possible role of this instability in experimental situations. We note that they are pressure driven modes and require the shear to be low in the regions of high pressure gradients. Experimentally it is well known that tokamaks are subject to sawtooth oscillations. It is believed that these oscillations result in a large region of low shear within the inversion radius often identified as the q=1 surface. If this picture of the q-profile is valid, than all sawtoothing

discharges are prime candidates for these low-n infernal modes. In addition to the lack of shear, a large enough pressure gradient is also required. This would imply that any instability would occur only at moderate to large values of β. There is recent evidence of unusual MHD behavior in connection with events such as giant sawteeth and β collapse. It would be interesting to analyze these discharges for a possible connection to infernal mode activity. Unfortunately, the experimental data rarely provides detailed information on the q-profile, a fundamental requirement for this sort of analysis. Finally we note that these instabilities may play a major role in ignited plasmas, where all the required plasma conditions may be present. To avoid them it will be necessary to maintain finite shear in the interior of the plasma or to broaden the pressure profile so that the pressure gradients are minimal in regions of low-shear.

Acknowledgments

REFERENCES

[1] Wesson, J.A., Nucl. Fusion 18 (1978) 87.

[2] Friedberg, J.P., Rev. Mod. Phys. 54 (1982) 801.

[3] Todd, A.M.M., Manickam, J., Okabayashi, M., Chance, M.S., Grimm, R.C., Greene, J.M., and Johnson, J.L., Nucl. Fusion 19 (1979) 743.

[4] Bernard, L.C., Moore, R.W., Phys. Rev. Lett. 46 (1981) 1286.

[5] Yamazaki, K., Amano, T., Naitou, H. Hamad, Y., Azumi, M., Nucl. Fusion 25 (1985) 1543.

[6] Kerner, W., Gautier, P., Lackner, K., Schneider, W., Gruber, R., Troyon, F., Nucl. Fusion 21 (1981) 1383.

[7] Greene, J.M., and Chance, M.S., Nucl. Fusion 21 (1981) 453.

[8] Manickam, J., Nucl. Fusion 24 (1984) 595.

[9] Chance, M.S., Jardin, S.C., and Stix, T.H., Phys. Rev. Lett. 51 (1983) 1963.

[10] Manickam, J., Grimm, R.C., and Okabayashi, M., Phys. Rev. Lett. 51 (1983) 1959.

[11] Dobrott, D., Nelson, D.B., Greene, J.M., Glasser, A.H., Chance, M.S., and Friedman, E.A., Phys. Rev. Lett. 39 (1977) 43.

[12] Connor, J.W., Hastie, R.J., and Taylor, J.B. Phys. Rev. Lett. 40 (1978) 396.

[13] Coppi, B., Ferreira, A., and Ramos, J.J., Phys. Rev. Lett. 44 (1980) 990.

[14] Grimm, R.C., Greene, J.M., and Johnson, J.L. Meth. Comp. Phys. 16 (1976) 253.

[15] Gruber, R., Troyon, F., Berger, D., Bernard, L.C., et al. Comp. Phys. Comm. 21 (1981) 323.

[16] Dewar, R.L., Manickam, J., Grimm, R.C., and Chance, M.S., Nucl. Fusion 21 (1981) 493.

[17] Charlton, L.A., Dory, R.A., Peng, Y.-K.M. Strickler, D.J., Lynch, S.J., et al. Phys. Rev. Lett 43 (1979) 1395.

[18] Taylor, J.B., Physikalische Blatter 35 (1979) 611.

[19] Hastie, R.J., and Taylor, J.B., Nucl. Fusion 21 (1981) 187.

[20] DeLucia, J., Jardin, S.C., and Todd, A.M.M., J. Comput. Phys. 37 (1980) 183.

Figure Captions

Fig. 1. Safety-factor profiles $q(\psi)$ used in this study. $q_{axis} = 1.05$, $q_{edge} = 3.10$ and α_q varying between 1.1 and 6.0.

Fig. 2. The pressure profile and its derivative corresponding to
   (a) $\alpha_1 = 4.0$, $\alpha_2 = 1.5$ used for most of the studies reported.
   (b) $\alpha_1 = 2.0$, $\alpha_2 = 6.0$ with the derivative shifted to the outside.

Fig. 3. (a) The variation of the growth rate (ω^2), arbitrary units, with the toroidal mode number, n, for the q-profile with $\alpha_q = 1.5$, $\beta = 0.8\%$. "B" marks the critical-n for marginal stability as determined by a WKB code.
   (b) Contours of constant growth rate, $\lambda(\psi,\theta_k)$, from the WKB code. The outermost contour signifies marginal stability, $\lambda = 0$.

Fig. 4. (a) ω^2 vs. n for $\alpha_q = 1.1$, $\beta = 1.5\%$, ω^2 is normalized in units of the poloidal Alfven frequency for this and subsequent figures.
   (b) Contours of $\lambda(\psi,\theta_k)$.

Fig. 5. (a) ω^2 vs. n for $\alpha_q = 1.5$, $\beta = 1.5\%$.
   (b) Contours of $\lambda(\psi,\theta_k)$.

Fig. 6. (a) ω^2 vs. n for $\alpha_q = 2.0$, $\beta = 1.5\%$.
   (b) Contours of $\lambda(\psi,\theta_k)$.

Fig. 7. (a) ω^2 vs. n for $\alpha_q = 2.5$, $\beta = 1.5\%$.

(b) Contours of $\lambda(\psi,\theta_k)$.

Fig. 8. (a) ω^2 vs. n for $\alpha_q = 3.0$, $\beta = 1.5\%$.

(b) Contours of $\lambda(\psi,\theta_k)$.

Fig. 9. (a) ω^2 vs. n for $\alpha_q = 4.0$, $\beta = 1.5\%$.

(b) Contours of $\lambda(\psi,\theta_k)$.

Fig. 10. (a) ω^2 vs. n for $\alpha_q = 6.0$, $\beta = 1.5\%$.

(b) Contours of $\lambda(\psi,\theta_k)$.

Fig. 11. (a) ω^2 vs. n for $\alpha_q = 4.0$ and the pressure profile of Fig. 2b. $\beta = 1.5\%$. The pressure profile is chosen to minimize the gradient in the region of low shear.

(b) Contours of $\lambda(\psi,\theta_k)$.

Fig. 12. (a) ω^2 vs. n for $\alpha_q = 6.0$ and the pressure profile of Fig. 2a, $\beta = 1.0\%$. This equilibrium is stable to high-n ballooning modes. The low-n modes are termed "infernal modes."

Fig. 13. The current density, pressure profiles and q-profiles for a model equilibrium that mimics typical experimental profiles. The units are arbitrary, q-axis = 1.05, q-edge = 3.1, and $\beta = 1.45\%$.

Fig. 14. (a) ω^2 vs. n for the equilibrium of Fig. 13, when $\beta = 1.45\%$.

(b) Contours of $\lambda(\psi,\theta_k)$.

Fig. 15. ω^2 vs. n for the equilibrium parameters of Fig. 13 with $\beta = 0.8\%$.,

showing the infernal modes where high-n is stable.

Fig. 16. ω^2 vs. n for the equilibrium of Fig. 15, with the toroidal field scaled so that q_{axis} is 0.96 instead of 1.05. Note the resonances of the instabilities with integer-n.

Fig. 17. The variation of the β limit with the shear parameter α_q for the infinite-n ballooning mode, and for the mode with n = 1.8. The region of instability for each mode lies above the corresponding curve. The hatched region identifies the domain of the infernal mode.

Fig. 18. A projection of the unstable displacement vector onto the x-z plane for the case with α_q = 3.0, β = 1.5%, and toroidal mode number n = 3.0.

Fig. 19. The displacement vector for the same equilibrium as Fig. 18, with toroidal mode number n = 7.0.

Fig. 20. Plots of $(q')^{-2}$ vs. ψ for different α_q. Standard ballooning theory is valid for n well above the appropriate curve.

87T0012

Fig. 1

#67T0011

Fig. 2

87T0017

Fig. 3

#87T0004

Fig. 4

#87T0008

(a)

(b)
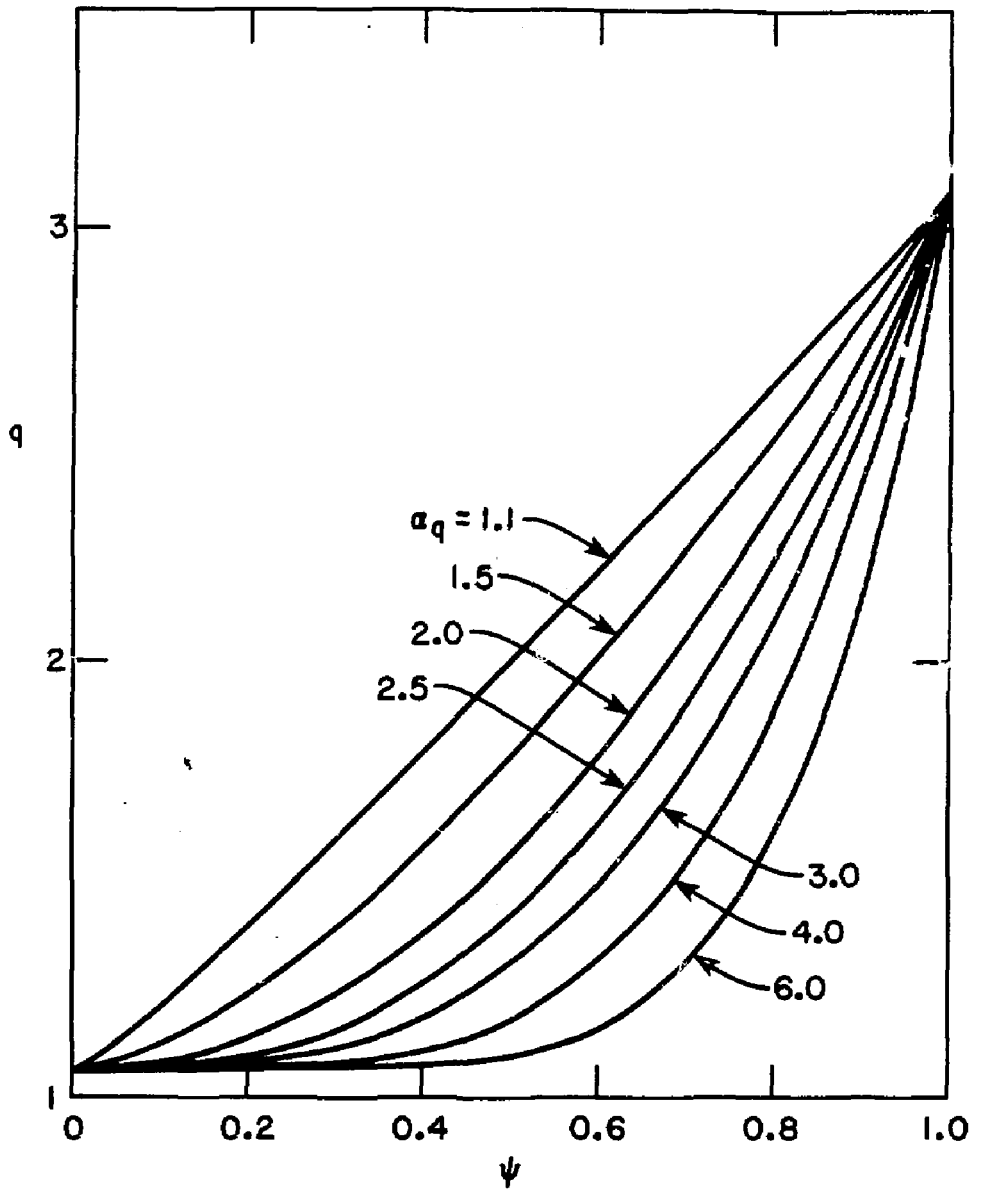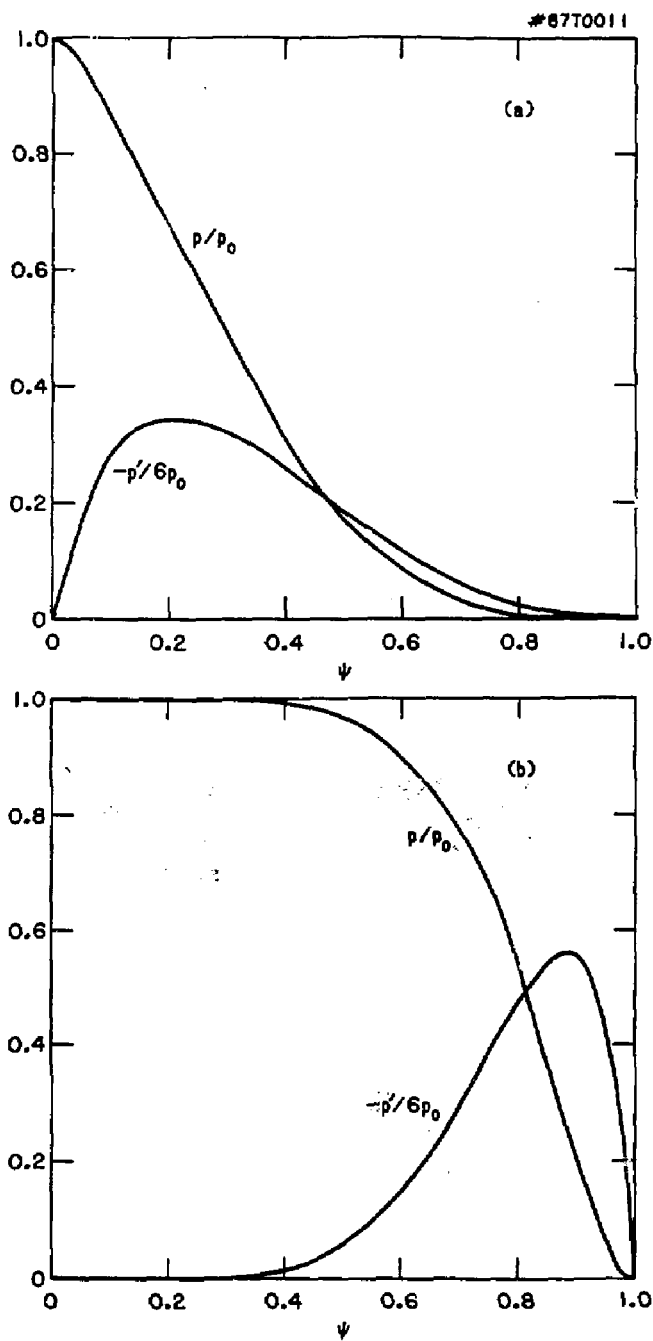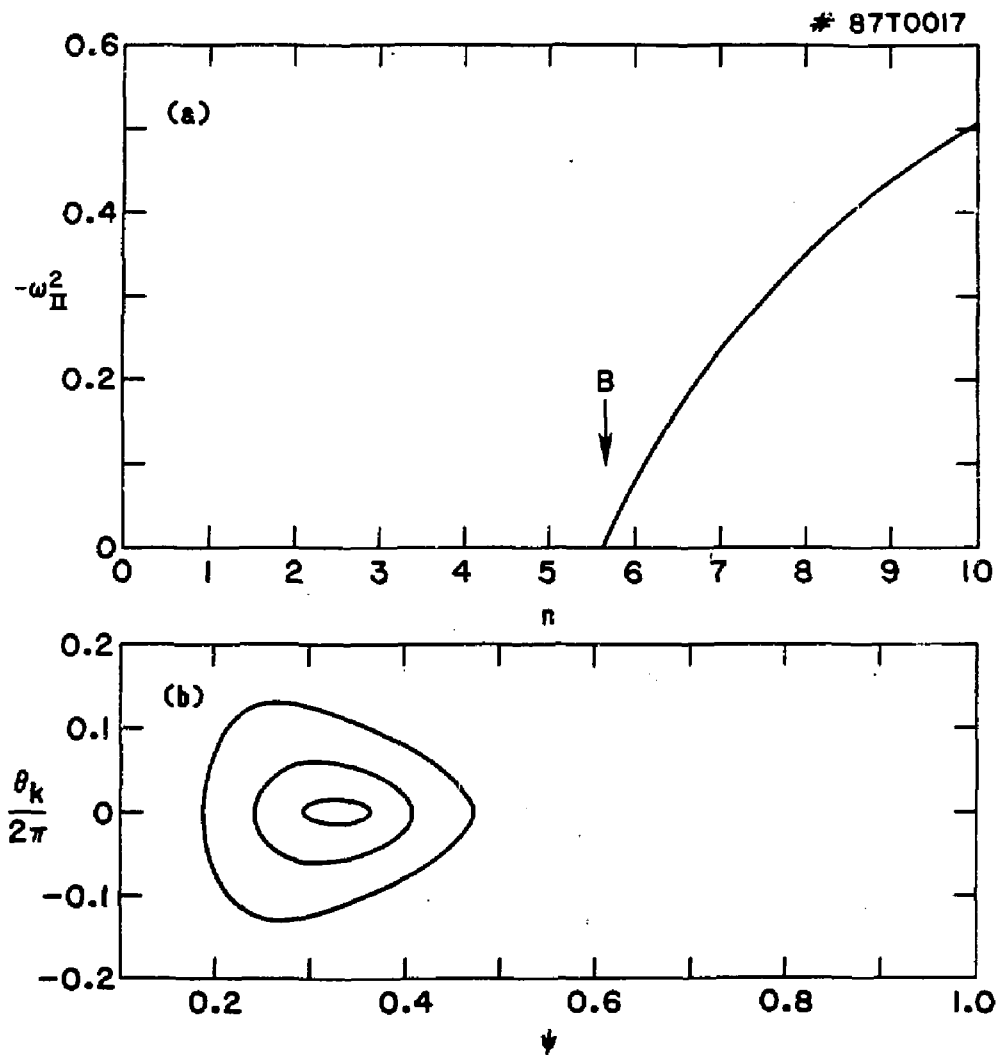
Fig. 5

#87T0001
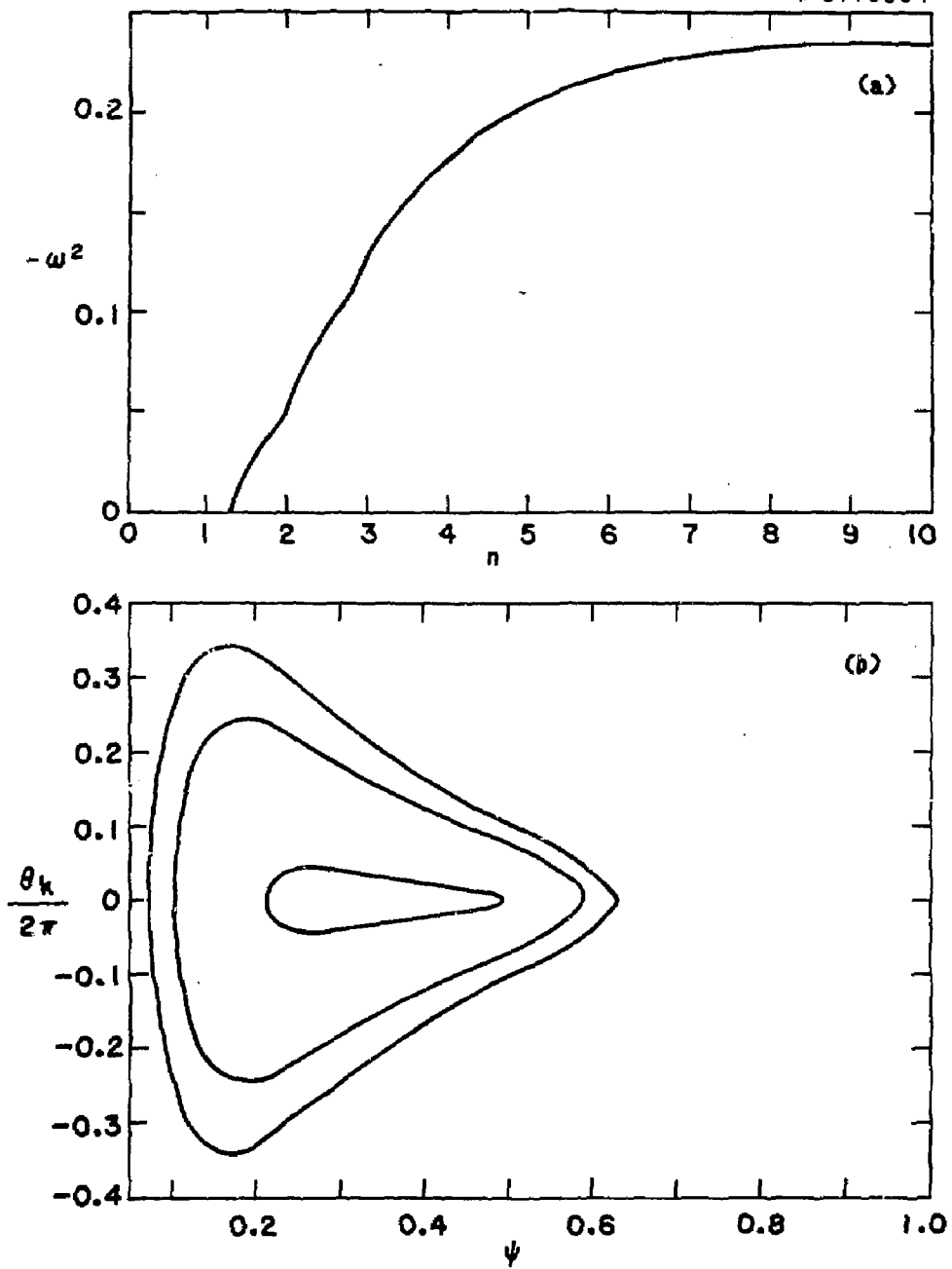
Fig. 6
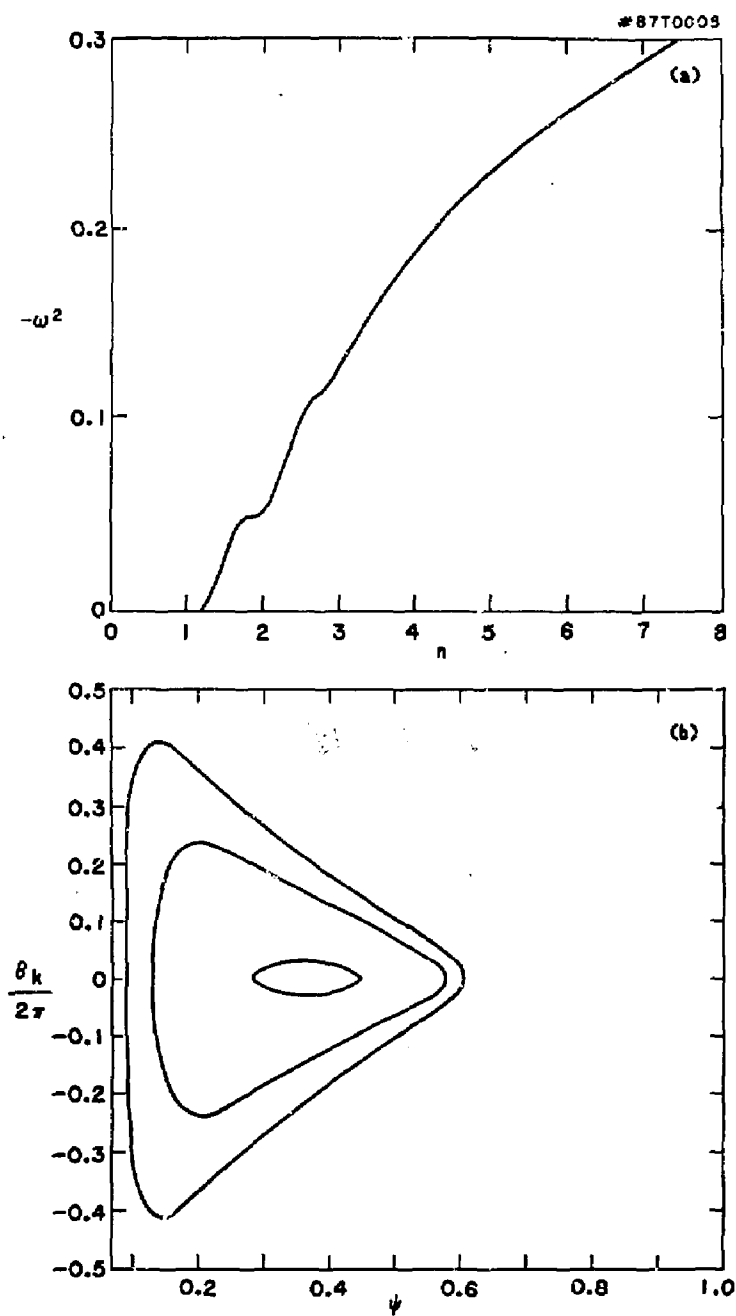
#87T0005
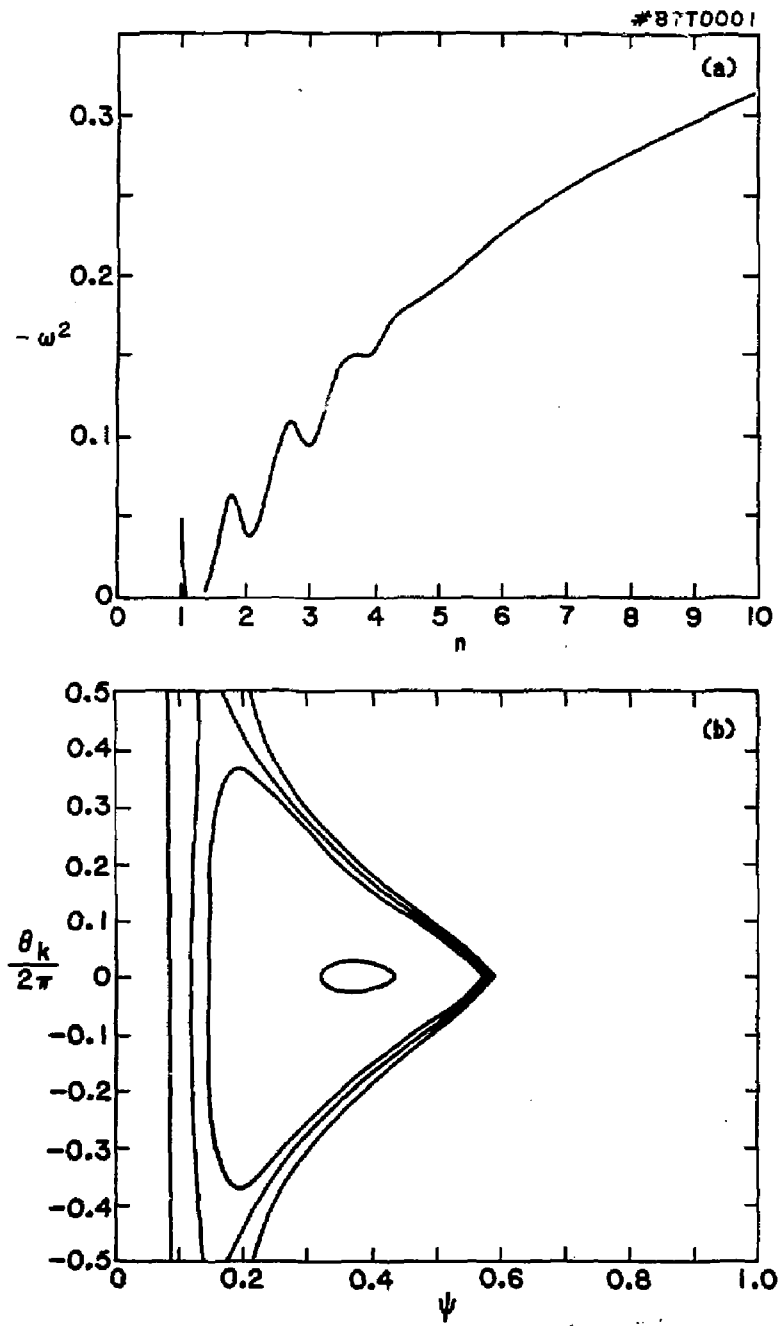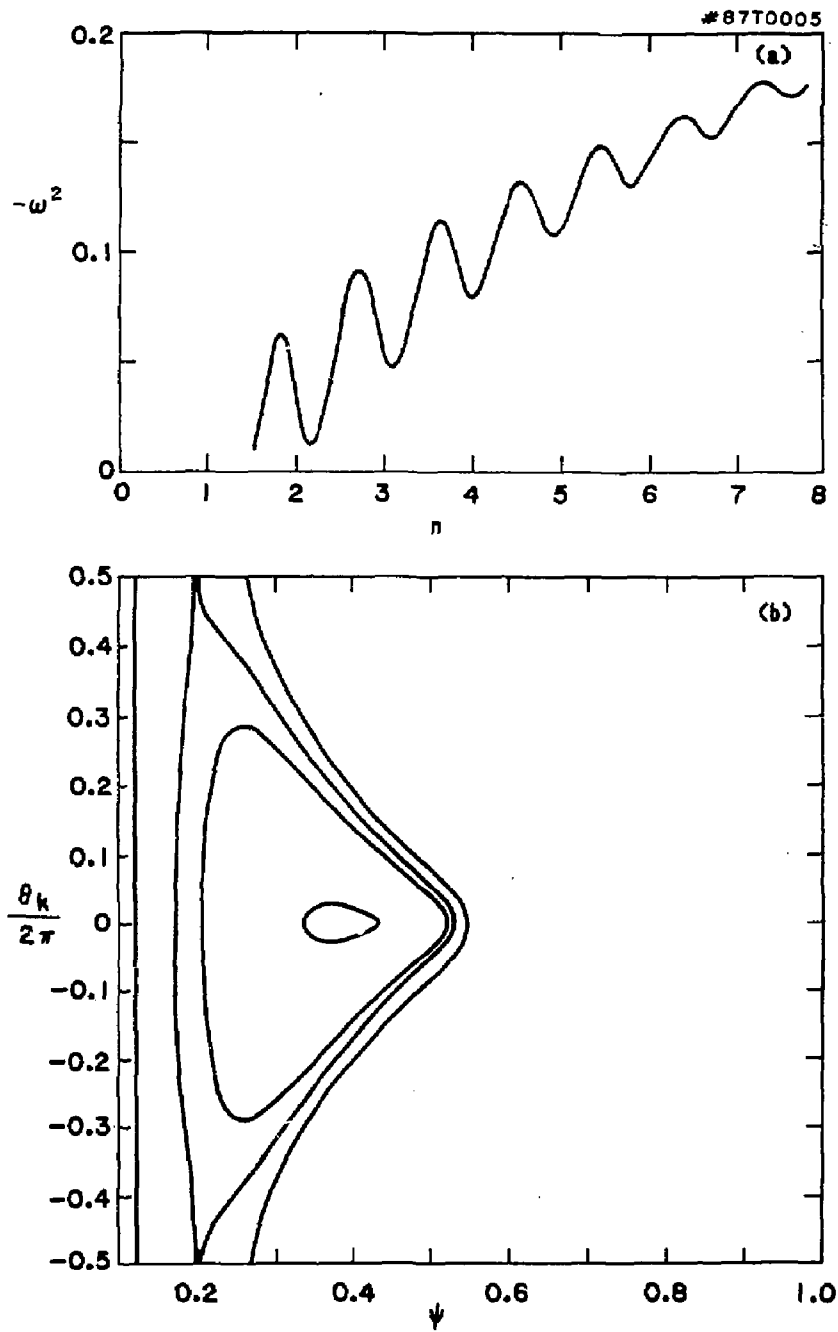
Fig. 7

#87T0010
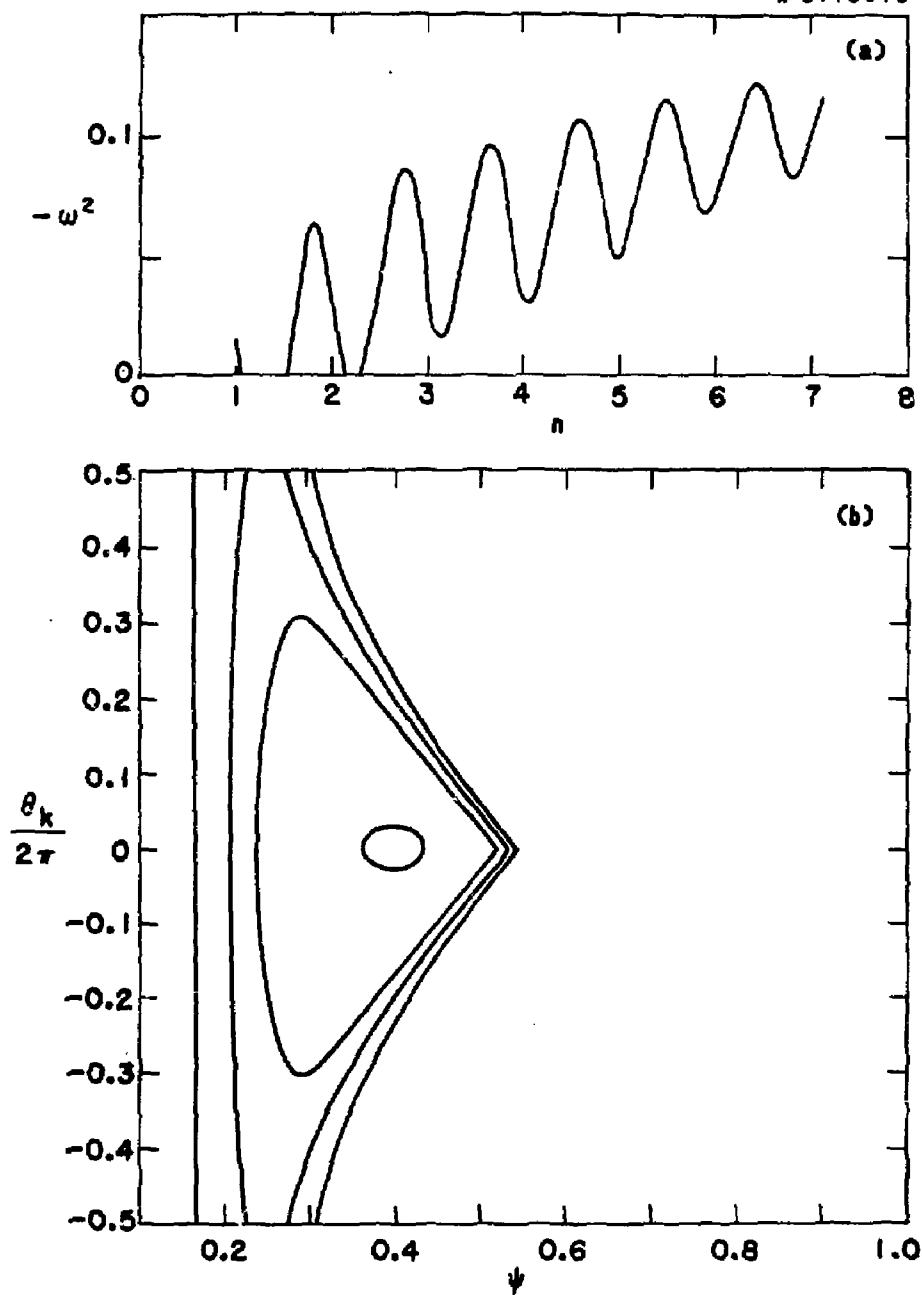
Fig. 8
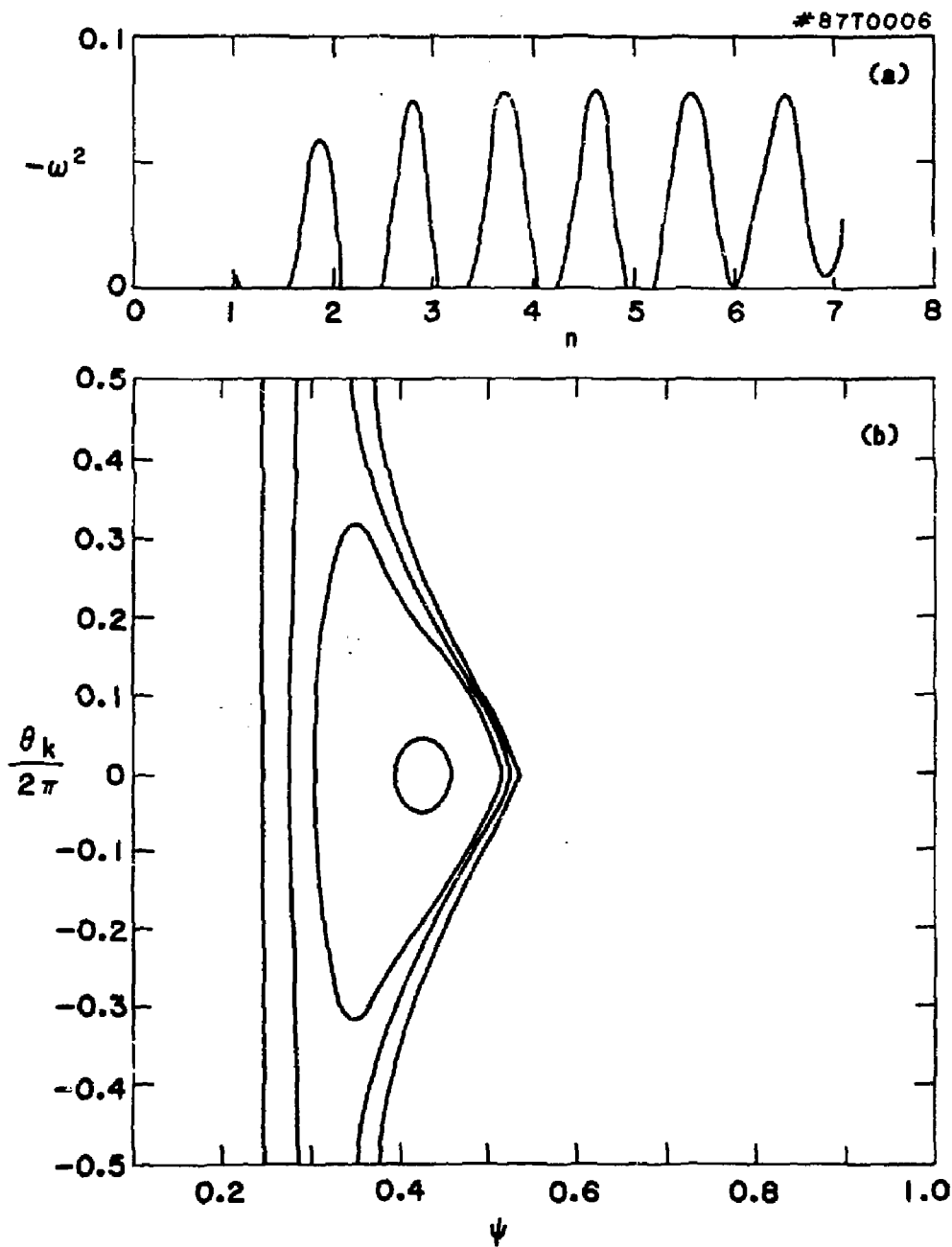
#87T0006

Fig. 9
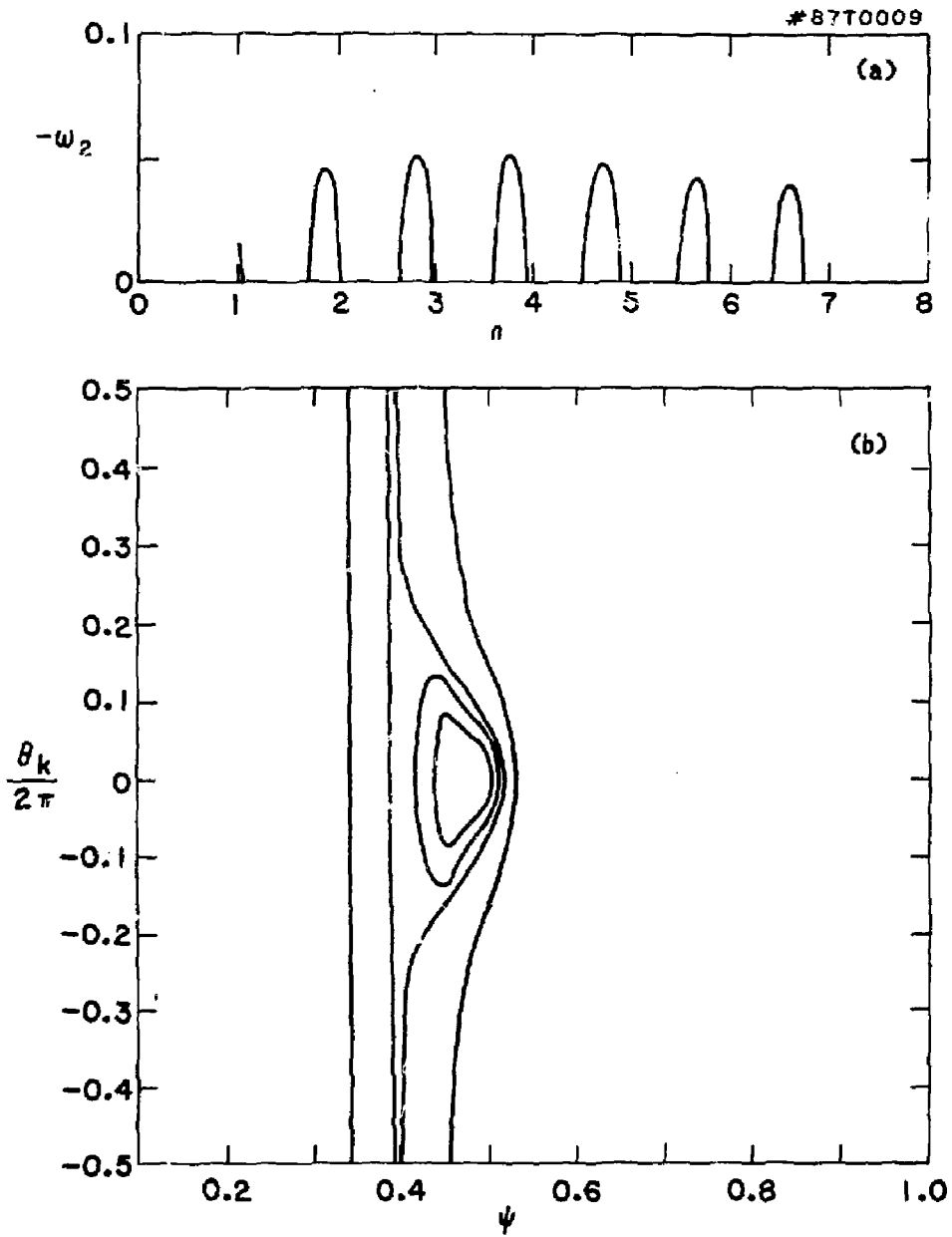
#87T0009

Fig. 10

#87T0007

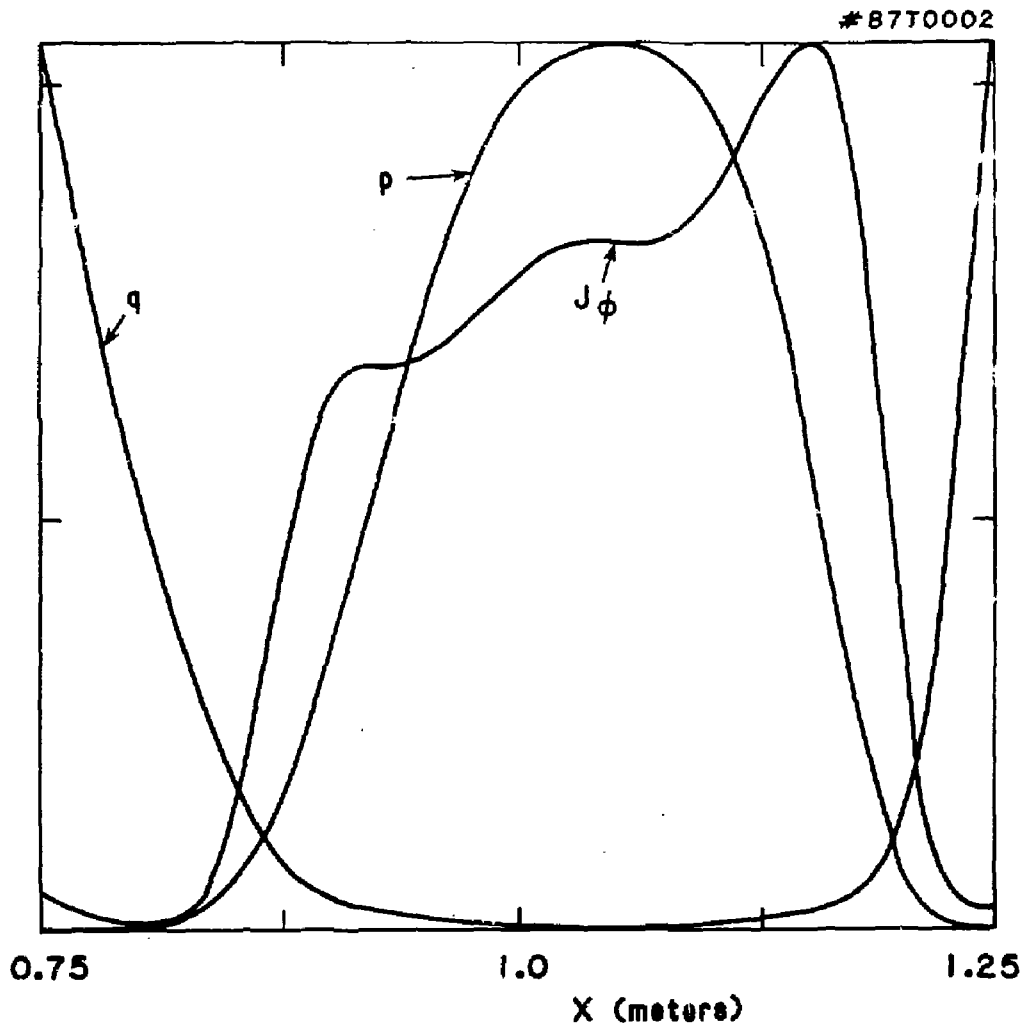Fig. 11

Fig. 12

#87T0002
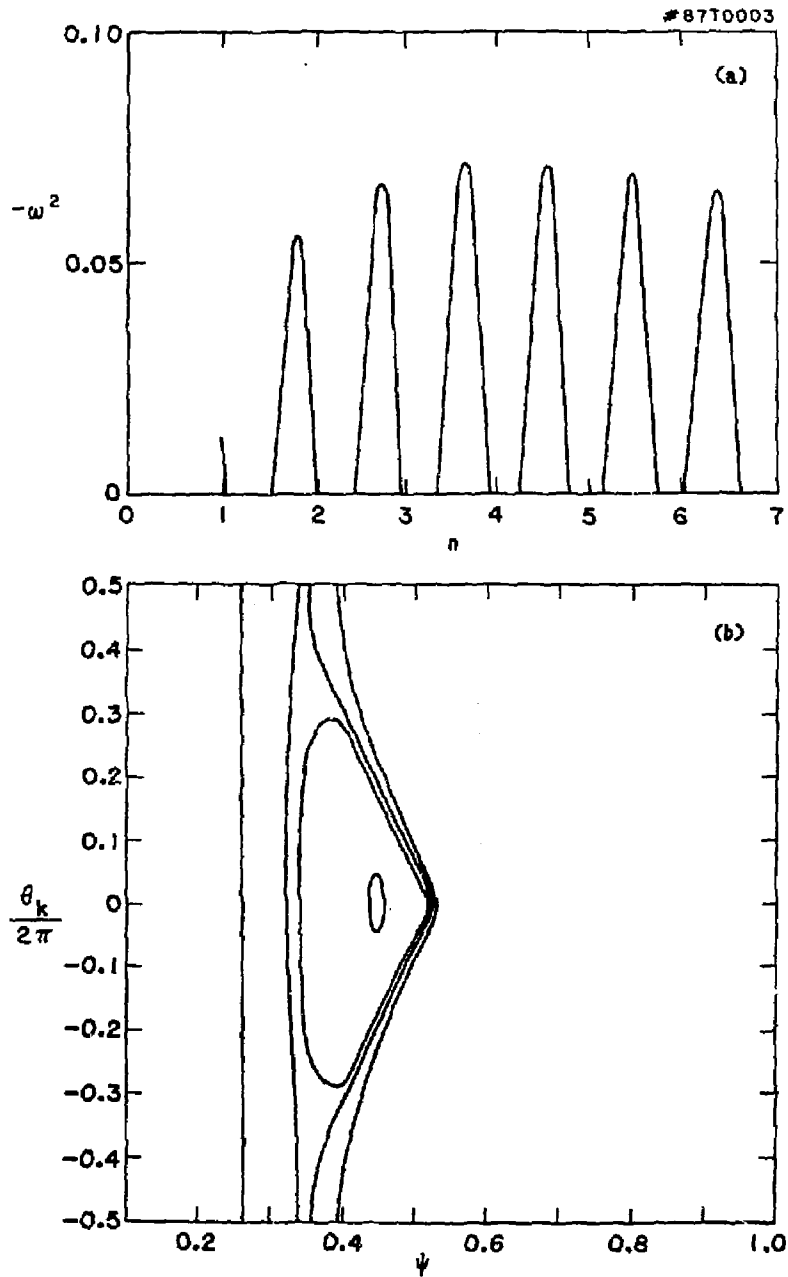

Fig. 13

#87T0003

(a)

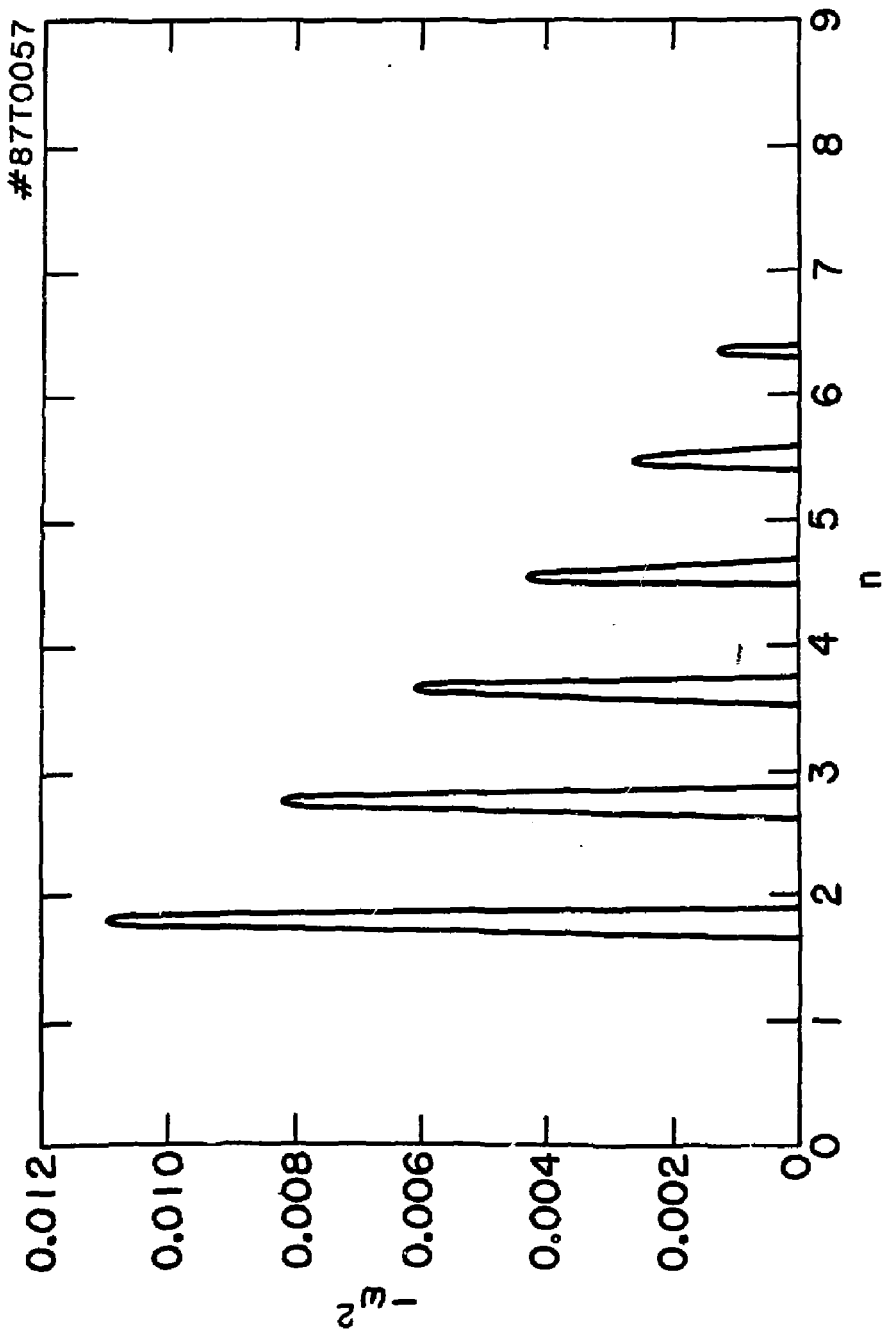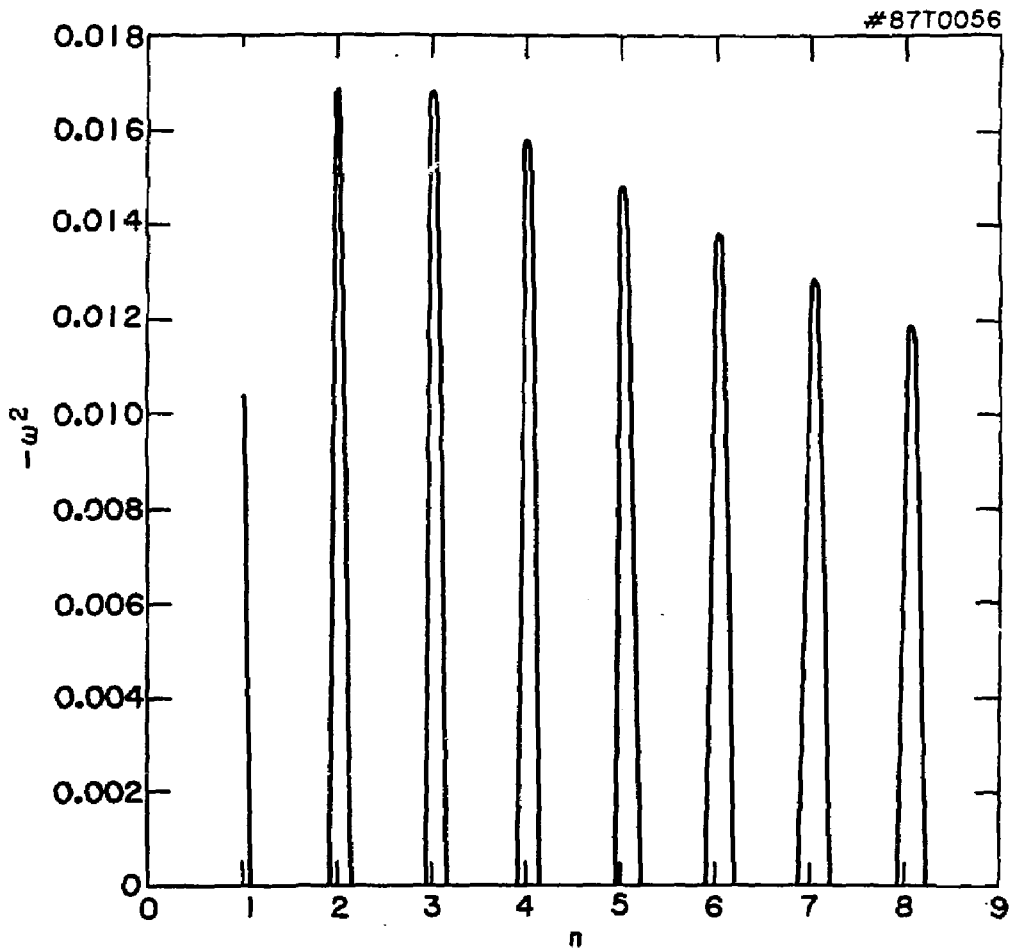$-\omega^2$

(b)

$\dfrac{\theta_k}{2\pi}$

ψ
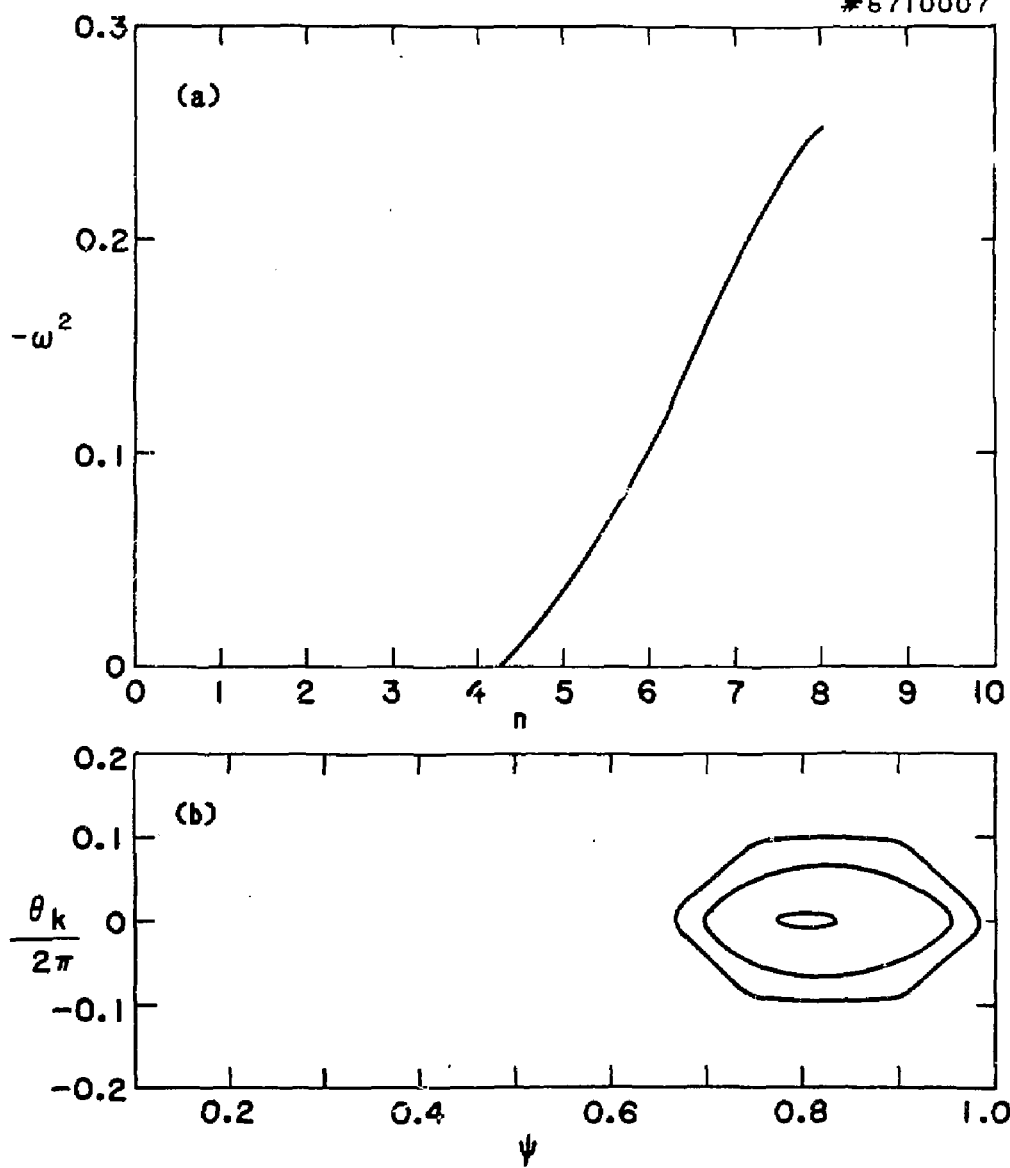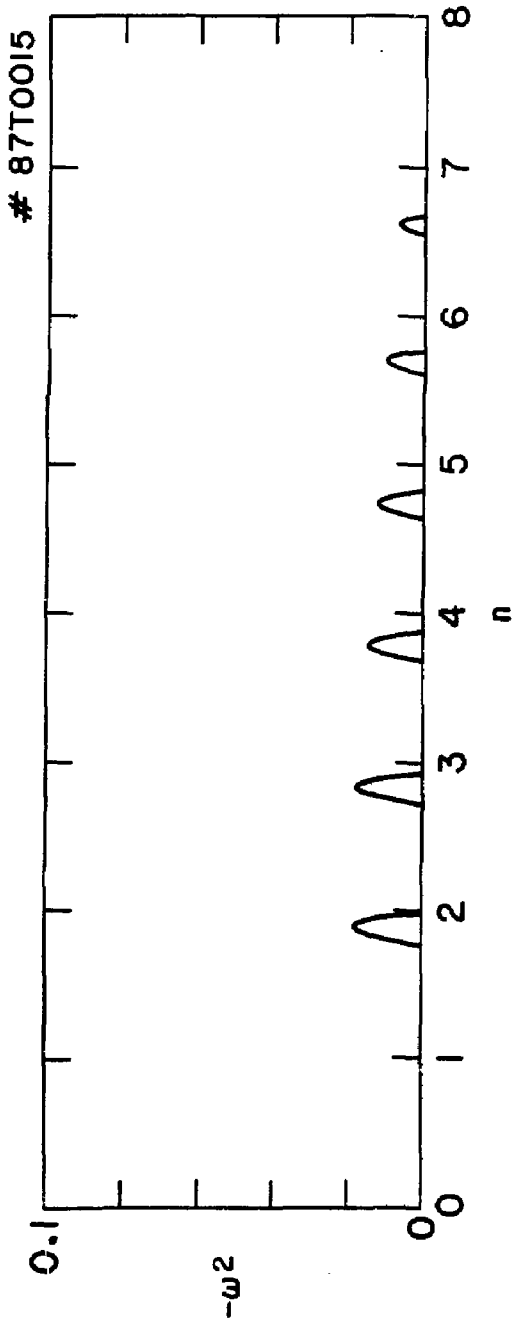
Fig. 14

Fig. 15

Fig. 16

87T0014
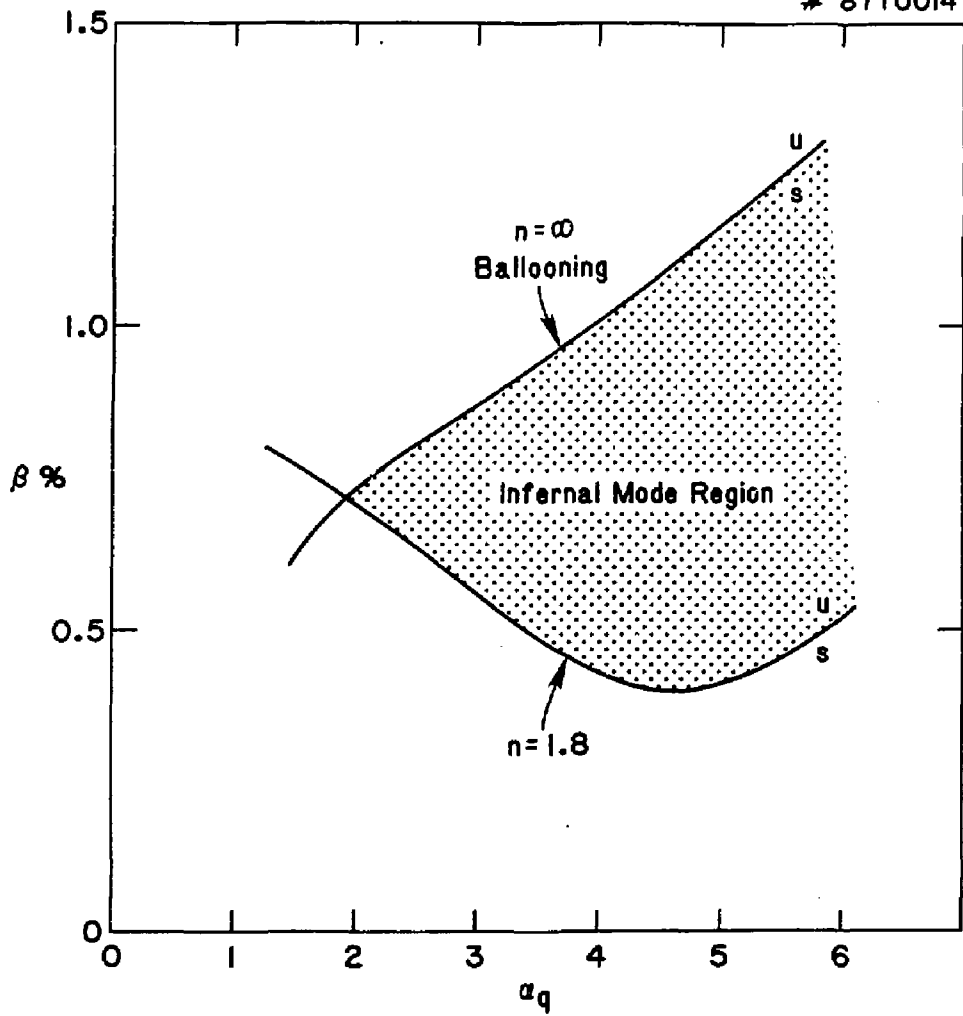
Fig. 17

87T0019
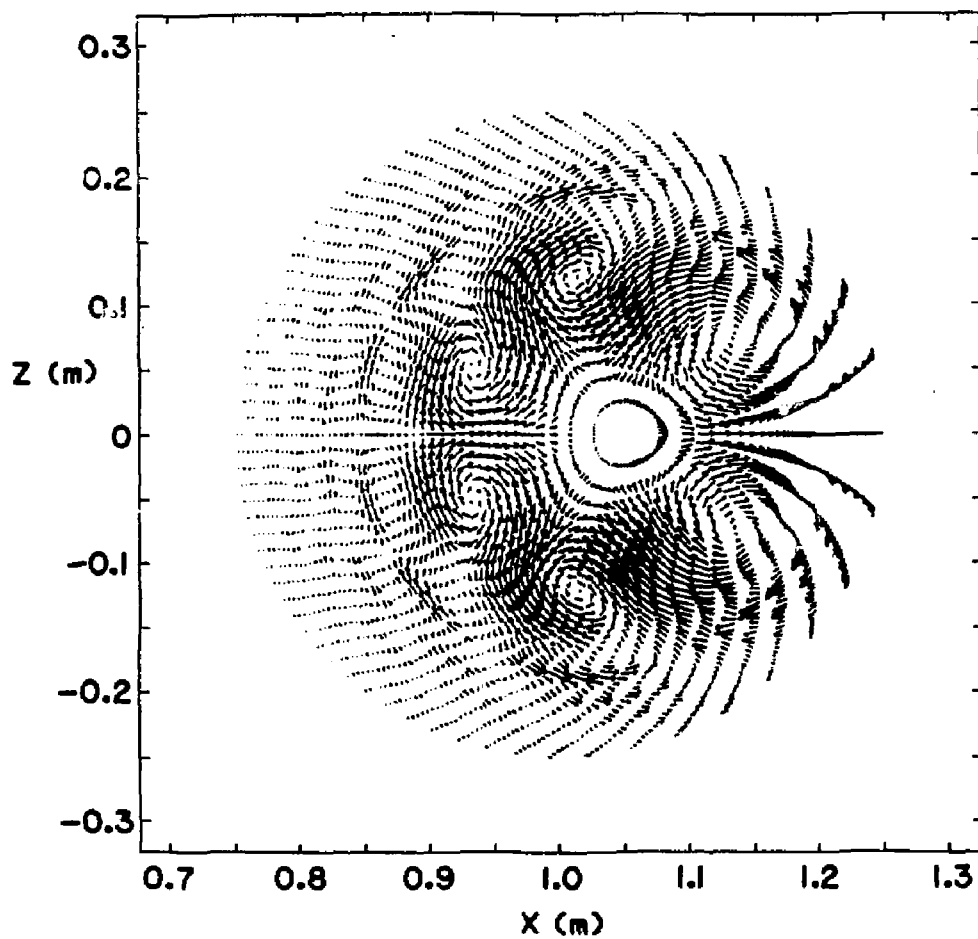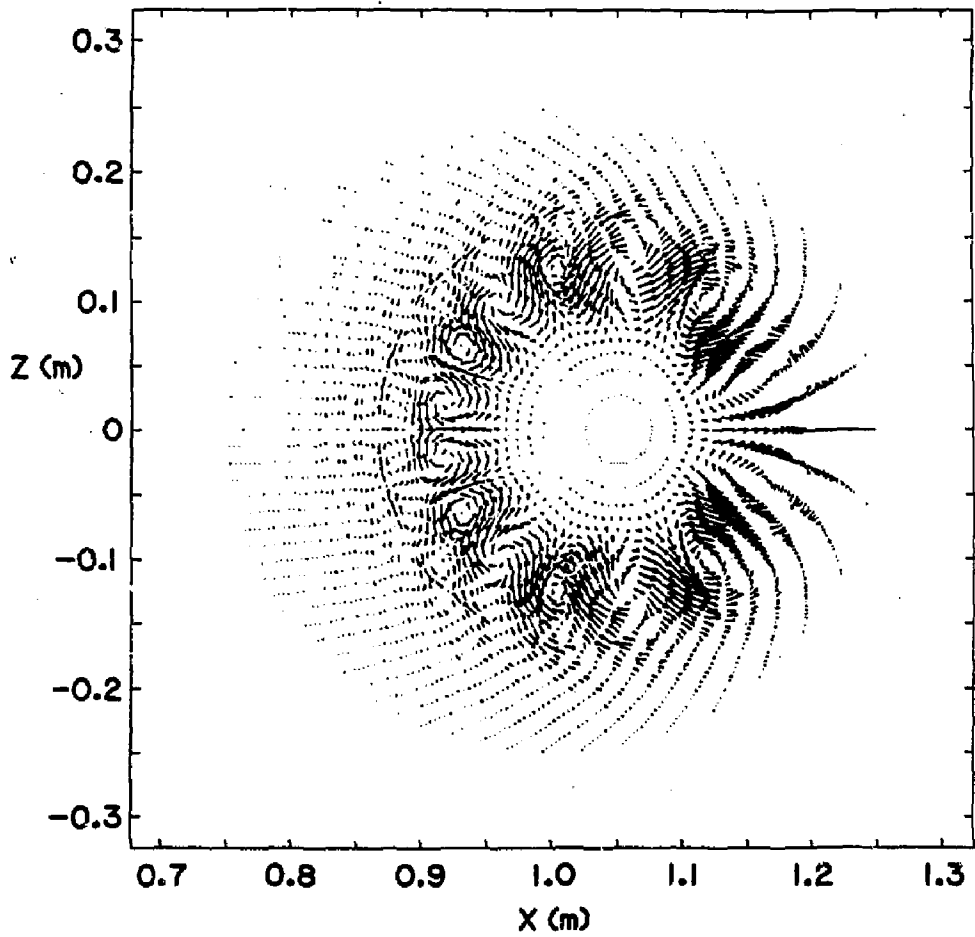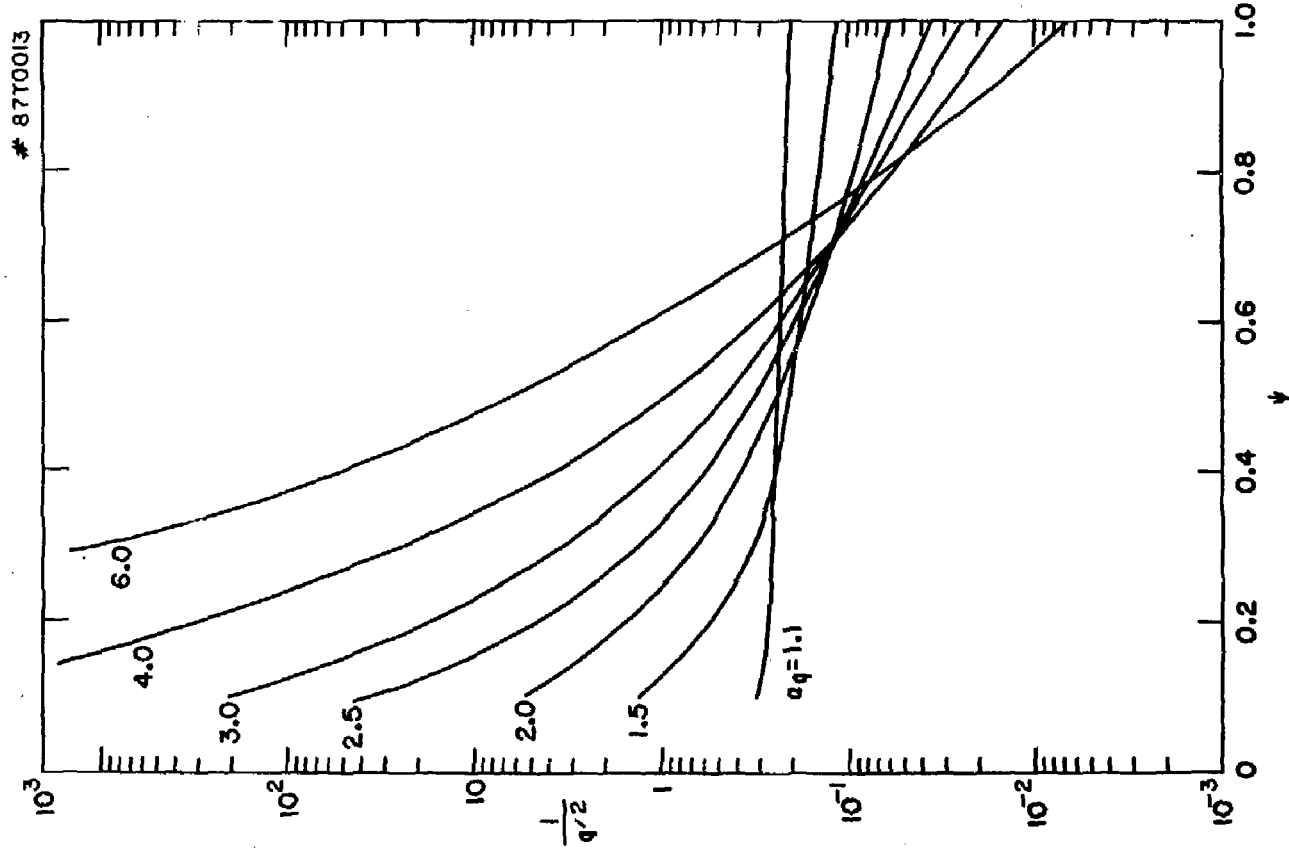

Fig. 18

87T0018

Fig. 19

Fig. 20

Dr. Frank J. Paoloni, Univ of Wollongong, AUSTRALIA
Prof. M.H. Brennan, Univ Sydney, AUSTRALIA
Plasma Research Lab., Australian Nat. Univ., AUSTRALIA
Prof. I.R. Jones, Flinders Univ., AUSTRALIA
Prof. F. Cap, Inst Theo Phys, AUSTRIA
Prof. M. Heindler, Institut fur Theoretische Physik, AUSTRIA
M. Goossens, Astronomisch Instituut, BELGIUM
Ecole Royale Militaire, Lab de Phys Plasmas, BELGIUM
Com. of European, Dg XII Fusion Prog, BELGIUM
Prof. R. Boucique, Laboratorium voor Natuurkunde, BELGIUM
Dr. P.H. Sakanaka, Univ Estadual, BRAZIL
Instituto De Pesquisas Espaciasi-INPE, BRAZIL
Library, Atomic Energy of Canada Limited, CANADA
Dr. M.P. Bachynski, MPB Technologies, Inc., CANADA
Dr. H.M. Skarsgard, Univ of Saskatchewan, CANADA
Dr. H. Barnard, University of British Columbia, CANADA
Prof. J. Teichmann, Univ. of Montreal, CANADA
Prof. S.R. Sreenivasan, University of Calgary, CANADA
Prof. Tudor W. Johnston, INRS-Energie, CANADA
Dr. C.R. James, Univ. of Alberta, CANADA
Dr. Peter Lukac, Komenskeho Univ, CZECHOSLOVAKIA
The Librarian, Culham Laboratory, ENGLAND
Mrs. S.A. Hutchinson, JET Library, ENGLAND
C. Mouttet, Lab. de Physique des Milleux Ionises, FRANCE
J. Radet, CEN/CADARACHE - Bat 506, FRANCE
Dr. Tom Mual, Academy Bibliographic, HONG KONG
Preprint Library, Cent Res Inst Phys, HUNGARY
Dr. B. Dasgupta, Saha Inst, INDIA
Dr. R.K. Chhajlani, Vikram Univ. INDIA
Dr. P. Kaw, Institute for Plasma Research, INDIA
Dr. Phillip Rosenau, Israel Inst Tech, ISRAEL
Prof. S. Cuperman, Tel Aviv University, ISRAEL
Librarian, Int'l Ctr Theo Phys, ITALY
Prof. G. Rostagni, Univ DI Padova, ITALY
Miss Clella De Palo, Assoc EURATOM-ENEA, ITALY
Biblioteca, del CNR EURATOM, ITALY
Dr. H. Yamato, Toshiba Res & Dev, JAPAN
Prof. I. Kawakami, Atomic Energy Res. Institute, JAPAN
Prof. Kyoji Nishikawa, Univ of Hiroshima, JAPAN
Direc. Dept. Lg. Tokamak Res, JAERI, JAPAN
Prof. Satoshi Itoh, Kyushu University, JAPAN
Research Info Center, Nagoya University, JAPAN
Prof. S. Tanaka, Kyoto University, JAPAN
Library, Kyoto University, JAPAN
Prof. Nobuyuki Inoue, University of Tokyo, JAPAN
S. Mori, JAERI, JAPAN
M.H. Kim, Korea Advanced Energy Research Institute, KOREA
Prof. D.I. Choi, Adv. Inst Sci & Tech, KOREA
Prof. B.S. Liley, University of Waikato, NEW ZEALAND
Institute of Plasma Physics, PEOPLE'S REPUBLIC OF CHINA
Librarian, Institute of Phys., PEOPLE'S REPUBLIC OF CHINA
Library, Tsing Hua University, PEOPLE'S REPUBLIC OF CHINA

Z. LI, Southwest Inst. Physics, PEOPLE'S REPUBLIC OF CHINA
Prof. J.A.C. Cabral, Inst Superior Tecn, PORTUGAL
Dr. Octavian Petrus, AL I CUZA University, ROMANIA
Dr. Johan de Villiers, Plasma Physics, AEC, SO AFRICA
Prof. M.A. Hellberg, University of Natal, SO AFRICA
Fusion Div. Library, JEN, SPAIN
Dr. Lennart Stenflo, University of UMEA, SWEDEN
Library, Royal Inst Tech, SWEDEN
Prof. Hans Wilhelmson, Chalmers Univ Tech, SWEDEN
Centre Phys des Plasmas, Ecole Polytech Fed, SWITZERLAND
Bibliotheek, Fom-Inst Voor Plasma-Fysica, THE NETHERLANDS
Dr. O.D. Ryutov, Siberian Acad Sci, USSR
Dr. G.A. Eliseev, Kurchatov Institute, USSR
Dr. V.A. Glukhikh, Inst Electro-Physical, USSR
Dr. V.T. Tolok, Inst. Phys. Tech. USSR
Dr. L.M. Kovrizhnykh, Institute Gen. Physics, USSR
Prof. T.J.M. Boyd, Univ College N Wales, WALES
Nuclear Res. Establishment, Julich Ltd., W. GERMANY
Bibliothek, Inst. Fur Plasmaforschung, W. GERMANY
Dr. K. Schindler, Ruhr Universitat, W. GERMANY
ASDEX Reading Rm, IPP/Max-Planck-Institut fur
   Plasmaphysik, W. GERMANY
Librarian, Max-Planck Institut, W. GERMANY
Prof. R.K. Janev, Inst Phys, YUGOSLAVIA